Clim Dyn (2014) 42:2411–2421
DOI 10.1007/s00382-013-1978-3

Variability of cloud liquid water and ice over South Asia from TMI estimates

A. Bhattacharya · A. Chakraborty · V. Venugopal

Received: 21 December 2012 / Accepted: 15 October 2013 / Published online: 2 November 2013

Abstract In this study, the Tropical Rainfall Measurement Mission based Microwave Imager estimates (2A12) have been used to compare and contrast the characteristics of cloud liquid water and ice over the Indian land region and the ocean surrounding it, during the premonsoon (May) and monsoon (June–September) seasons. Based on the spatial homogeneity of rainfall, we have selected five regions for our study (three over ocean, two over land). Comparison across three ocean regions suggests that the cloud liquid water (CLW) over the orographically influenced Arabian Sea (close to the Indian west coast) behaves differently from the CLW over a trapped ocean (Bay of Bengal) or an open ocean (equatorial Indian Ocean). Specifically, the Arabian Sea region shows higher liquid water for a lower range of rainfall, whereas the Bay of Bengal and the equatorial Indian Ocean show higher liquid water for a higher range of rainfall. Apart from geographic differences, we also documented seasonal differences by comparing CLW profiles between monsoon and premonsoon periods, as well as between early and peak phases of the monsoon. We find that the CLW during the lean periods of rainfall (May or June) is higher than during the peak and late monsoon season (July–September) for raining clouds. As active and break phases are important signatures of the monsoon progression, we also analysed the differences in CLW during various phases of the monsoon, namely, active, break, active-to-break and break-to-active transition phases. We find that the cloud liquid water content during the break-to-active transition phase is significantly higher than during the active-to-break transition phase over central India. We speculate that this could be attributed to higher amount of aerosol loading over this region during the break phase. We lend credence to this aerosol-CLW/rain association by comparing the central Indian CLW with that over southeast Asia (where the aerosol loading is significantly smaller) and find that in the latter region, there are no significant differences in CLW during the different phases of the monsoon. While our hypothesis needs to be further investigated with numerical models, the results presented in this study can potentially serve as a good benchmark in evaluating the performance of cloud resolving models over the Indian region.

Keywords Cloud microphysics · Hydrometeors · Precipitation · Aerosols · Active and break monsoon

1 Introduction

The latent heat released during formation of clouds plays a major role in the tropical and extratropical weather (Matsuno 1966; Webster 1972). The various types of precipitating clouds have different kinds of heating structures (Houze 1982), with the amount of latent heat release or absorption depending on the type of phase change, viz., melting, freezing, condensation, evaporation, sublimation and deposition. Hence the vertical distribution of latent heat carries the signatures of the various phases of water present at different heights (Zuluaga et al. 2010). However, accurate estimation of cloud liquid water (CLW) and cloud ice (CLI) phase hydrometeors remains a challenge. Noh and Haar (2009) utilized intensive aircraft in situ observations and various satellite data to compare model simulation results. In recent years, Cloudsat satellite data have been used to measure the vertical structure of clouds and

A. Bhattacharya · A. Chakraborty (✉) · V. Venugopal
Centre for Atmospheric and Oceanic Sciences, Indian Institute of Science, Bangalore 560012, India
e-mail: arch@caos.iisc.ernet.in

precipitation from space (Noh and Haar 2009; Marchand et al. 2008; Luo et al. 2009).

The Tropical Rainfall Measurement Mission (TRMM) Microwave Imager (TMI) and Precipitation Radar (PR) are flown aboard the TRMM satellite. While PR measures reflectivity, TMI measures the brightness temperature and uses an algorithm (Kummerow et al. 2001) to estimate the rain rate and other variables. The TRMM 2A12 dataset, a TMI product, gives precipitation water, precipitation ice, cloud water, cloud ice, rain rate, and latent heat. There are disagreements between rainfall estimates from the TMI and PR for certain regions (Tao et al. 2001; Dinku and Anagnostou 2005; Gopalan et al. 2010). However, over continental regions and Atlantic Ocean, rainfall is found to be identical from these two datasets (Tao et al. 2001). Berg et al. (2006) proposed an algorithm which reduces the root mean square difference of rainfall estimates from TMI and PR by approximately 75 %. These biases have been found to be higher for warm season convective zones and semi-arid regions. The difference is found to be significant for extremely low rain rates (less than 2 mm/h); however for higher rain rates the difference diminishes (Wang et al. 2009; Olson et al. 2006). By comparing the vertical and horizontal cross sections of cloud liquid water, ice and precipitation water over land and ocean, Masunaga et al. (2002) showed that CLW estimates from PR exceed TMI in mid-latitude winter, but TMI estimates exceed PR around the tropical rainfall maximum. Typically, the brightness temperature-rainrate relation holds good for most precipitation systems in different seasons and over various land regions (Gopalan et al. 2010). An additional source of confidence in the 2A12 estimates is that the two derived latent heat datasets (TRMM Convective and Stratiform Heating (CSH) and TMI 2A12) are in agreement in terms of magnitude and level of maximum heating (Zuluaga et al. 2010).

The vertical structure of hydrometeors (and the associated latent heat) over the Indian region and the surrounding oceans has not been studied extensively due to limited observations. In a related study, Zuluaga et al. (2010) documented the four-dimensional latent heat structure over the south Asian monsoon region. They reported an ocean and land contrast in latent heat, and the heavy precipitation produced by the complex terrain. They also found that a spatial dipole of latent heat anomalies occurs between the equatorial Indian Ocean and the Bay of Bengal regions during active and break phases of monsoon intraseasonal oscillations. In a more recent study, Halder et al. (2012) documented a lead-lag relationship between hydrometeors and surface precipitation during the monsoon period, using TRMM 2A12 and 3B42 data.

The recent availability of high-resolution satellite observations and *in situ* observations arising out of field campaigns over India, along with improved numerical models, provide an ideal avenue to document and understand the vertical structure of hydrometeors over the Indian region. The objective of this study is to identify and systematically document the signatures of the vertical structure of cloud liquid water and cloud ice hydrometeors over the Indian land region and the surrounding oceans. In Sect. 2, we provide a description of the TRMM 2A12 data used for our analysis. Section 3 discusses the main results of our observational analysis, followed by a summary in Sect. 4.

2 Data

This study uses CLW, CLI and precipitation from TRMM 2A12 version 6 product. The product is generated based on a Bayesian retrieval scheme, for which *a priori* knowledge is created using an ensemble of cloud resolving model simulations. Over the oceans, due to lack of completeness and representativeness of the data, the methodology is not generally considered reliable. As shown by Kummerow et al. (2011), the 2A12 dataset has a large bias, especially close to the Equator, where sea surface temperature and atmospheric water vapour generally are high.

The 2A12 V6 product is available from the sea level to a height of 18 km, divided into 14 vertical levels. The vertical resolution of the data set varies with height, with 0.5 km separation from surface to 4 km, 1 km separation from 4 to 6 km, 2 km apart from 6 to 10 km and 4 km separation above 10 km. The horizontal resolution of this data is about 4.4×4.4 km^2 over 759 km wide swath for which instantaneous snapshots are available (approximately 15 per day) from December 1997 through August 2001. After August 2001, due to a change in the orbit, the data resolution changed to 5.1×5.1 km^2 over 858 km wide swath. Each pixel of the 2A12 product was relocated to $0.05^\circ \times 0.05^\circ$ regular grid that holds the centre of the pixel. Any data gaps after this relocation were filled by bilinear interpolation. The spatial pattern as well as the intensity of different parameters (CLW, CLI, precipitation) in the regridded dataset were similar to those before re-gridding. In this study we have used data for premonsoon (May) and monsoon seasons (June–September) of the years 2004–2010.

Figure 1a shows the mean surface precipitation (mm/day) from TRMM 2A12 estimates during JJAS 2004–2010. High precipitation over northern Bay of Bengal, along the western parts of the Western Ghats mountains and just south of the Equator correspond well with other estimates (e.g., TRMM 3B42; not shown). It has also realistically captured the low precipitation region off the south-eastern parts of the Indian peninsula. We find that the spatial correlation between the 2A12 and

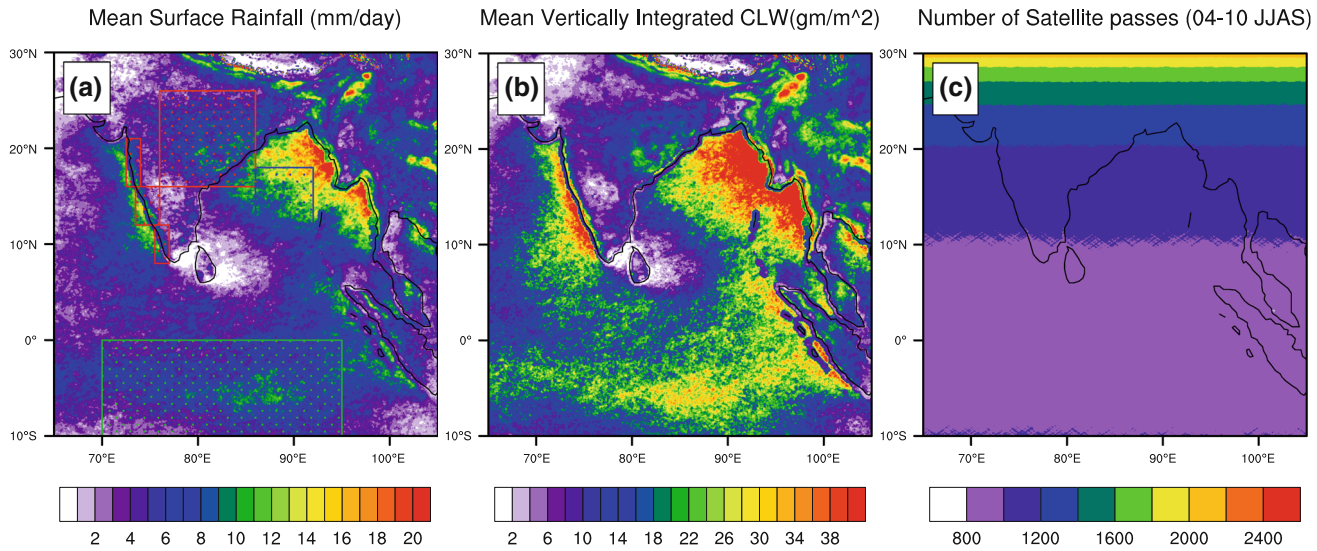

Fig. 1 **a** Mean surface rainfall (mm/day); and **b** Mean vertically integrated CLW (gm/m^2) during JJAS of 2004–2010 from TRMM 2A12 estimates. Boxes shown in panel (**a**) indicate regions used for further study: Bay of Bengal (86°–92° E, 12°–18° N), Central India (only land, 76°–86° E, 16°–26° N), Equational Indian Ocean (70°–95° E, 10° S-Eq), West Coast Ocean and West Coast Land (boxes along west coast of Indian peninsula, ocean and land parts respectively). **c** Number of satellite passes over every grid in the region during JJAS 2004–2010

3B42 V6 (gridded, 0.25-degree) seasonal precipitation climatology is 0.75. The vertically integrated CLW (gm/m^2) during the same period (Fig. 1b) shows, as expected, a close resemblance to surface precipitation. CLW values are high over north Bay of Bengal, western parts of the Indian peninsula and over equatorial Indian Ocean. These places are associated with high amount of JJAS precipitation as seen in Fig. 1a. The spatial correlation between climatological rainfall and vertically integrated CLW is 0.94. Finally, Fig. 1c shows the total number of satellite passes over each grid box over our study region. During this period (JJAS of 2004–2010) the number of satellite passes were at least 800 at any grid point in our selected domain. The number increases with the latitude over this selected domain because of the path of the TRMM polar orbiting satellite. Therefore, Fig. 1a and b represent robust climatological spatial distributions of precipitation and CLW, respectively.

3 Results

Based on Fig. 1, we identify five regions (3 over ocean and 2 over land) which exhibit homogeneity in the spatial distribution of climatological precipitation and CLW. These five regions are Bay of Bengal (BoB), Central India (CI), Equatorial Indian Ocean (EIO) West Coast Land (WCL), and West Coast Ocean (WCO), shown as rectangular boxes in Fig. 1a. Their spatial extents are defined in Table 1. Even though the central Indian region, as considered, includes a portion of BoB, all estimates are done only using the land portion of the CI box. The five regions selected have different characteristics, in terms of total precipitation and geography. Specifically, among the three ocean regions, we have an open ocean (EIO), a trapped ocean (BoB) and an ocean influenced by orography (WCO), and among the land regions, one is mostly plains (CI) and the other influenced by orography (WCL).

Table 1 The spatial extent of the five land and ocean regions selected for analysis

Region	Location	Land/Ocean
Bay of Bengal (BoB)	(86°–92°E, 12°–18°N)	Ocean
Central India (CI)	(76°–86°E, 16°–26°N) (Only land portion)	Land
Equatorial Indian Ocean (EIO)	(70°–95°E, 10°S-Eq)	Ocean
West Coast Ocean (WCO)	(72.5°–74°E, 16°–21°N) (73.5°–76°E, 12°–16°N) (75.5°–77°E, 8°–12°N)	Ocean
West Coast Land (WCL)	(72.5°–74°E, 16°–21°N) (73.5°–76°E, 12°–16°N) (75.5°–77°E, 8°–12°N)	Land

3.1 Geographical differences

Figures 2a, b show the climatological mean of CLW and CLI (in gm/m^3), respectively, from all the orbital data for June–September (JJAS) of 2004–2010 in the five selected

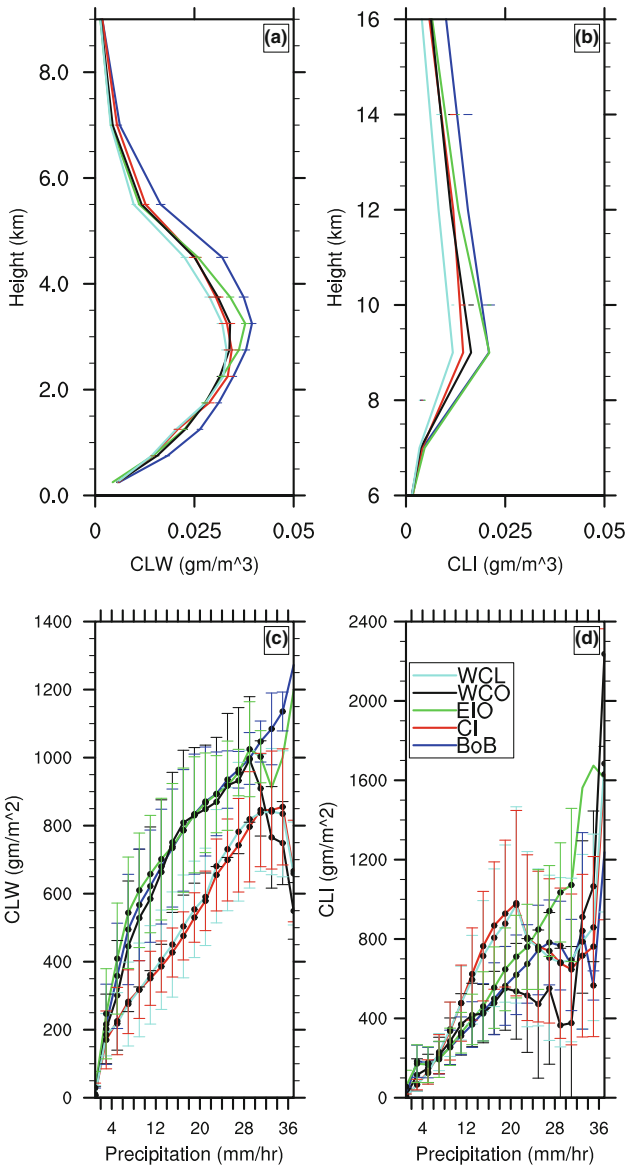

Fig. 2 (*Top row*) Climatological (JJAS 2004–2010) **a** mean cloud liquid water and **b** mean cloud ice (in gm/m^3) over the five regions shown in Fig. 1. The yearly standard deviations are represented by horizontal bars. (*Bottom row*) Vertically integrated **c** CLW; and **d** CLI (in gm/m^2), as a function of precipitation, over the five regions. The precipitation values have been grouped into 2 mm/h bins. The standard deviations estimated for each precipitation bin are shown as *vertical bars*

regions, with the respective interannual variability shown as bars. In estimating the mean CLW or CLI, we consider only those locations which have measurable surface precipitation. This was done to avoid bias in mean CLW values depending on the frequency of occurrence of non-rainy grids over a region. It is evident from Fig. 2a that the mean CLW varies with height, with almost no concentration above 9 km from the surface. The highest value of mean CLW occurs around a height of 2–3 km for the two land regions, namely, Central India and West Coast Land (Fig. 2a). On the other hand, the CLW over ocean regions (trapped or open) has a maximum at a height of around 3 km. The difference in the peak value of CLW between land and oceanic regions might partially be due to biases (particularly over ocean regions) in the 2A12 data set. That said, a comparison of JJAS outgong longwave radiation between central India and the Bay of Bengal (figure not shown) suggests that deeper convection is more prominent over the latter region (ocean) compared to the former (land). Thus, it could very well also be a regional characteristic. The relative contribution of the bias and regional behavior to the observed ocean-land contrast is an issue that needs further investigation. Although the West Coast Ocean region has a lower mean CLW compared to BoB (trapped) or EIO (open) regions, it also shows a maxima at 3 km. In contrast to CLW, CLI does not show any substantial variation with height; this apparent lack of structure in CLI in comparison to CLW might have to do with the coarsening vertical resolution in TRMM 2A12, as one goes to the upper levels. That said, the CLI profiles over land and ocean regions group themselves, as in the case of CLW, with possible (although weak) maximum at 9 km.

In order to understand the dependence of CLW with precipitation, we estimate the vertically integrated cloud liquid water and ice as a function of surface precipitation rate. The JJAS climatology (2004–2010) of this precipitation dependence is shown in Fig. 2c, d. Yet again, we observe that the CLW over land and ocean group themselves into two distinct categories (despite the high standard deviations, shown as bars, at the high precipitation intensities), with the CLW over ocean in general being higher than that over the land region for most of the precipitation rates. The CLI profiles of land and ocean also appear distinct; however, the behaviour of CLI is more complex, with a hint of separation between land and ocean regions, up to 20 mm/hr. Beyond 20 mm/hr, the ocean CLI profiles appear to diverge, with the open ocean (EIO, in Fig. 2d) showing a significantly higher CLI than BoB or WCO. Whether this rapid increase in CLI over EIO can be attributed completely to the known (large) biases of TRMM 2A12 over the equatorial region (Kummerow et al. 2011) is an issue that needs further investigation.

Combining the vertical and precipitation dependence, Fig. 3 shows the vertical profiles of CLW and CLI as a function of precipitation intensity for the five selected regions. In general, the CLW increases up to 5 km over the ocean (e.g., Fig. 3c, e). Above 6 km it decreases for all precipitation intensities. However, over land, CLW is very low in the lower atmosphere, and gradually increases till 4–5 km, where it reaches a maximum, and then decreases (Fig. 3a, i). In addition, over land, for higher precipitation intensities (>25 mm/hr), CLW has two distinct peaks (in

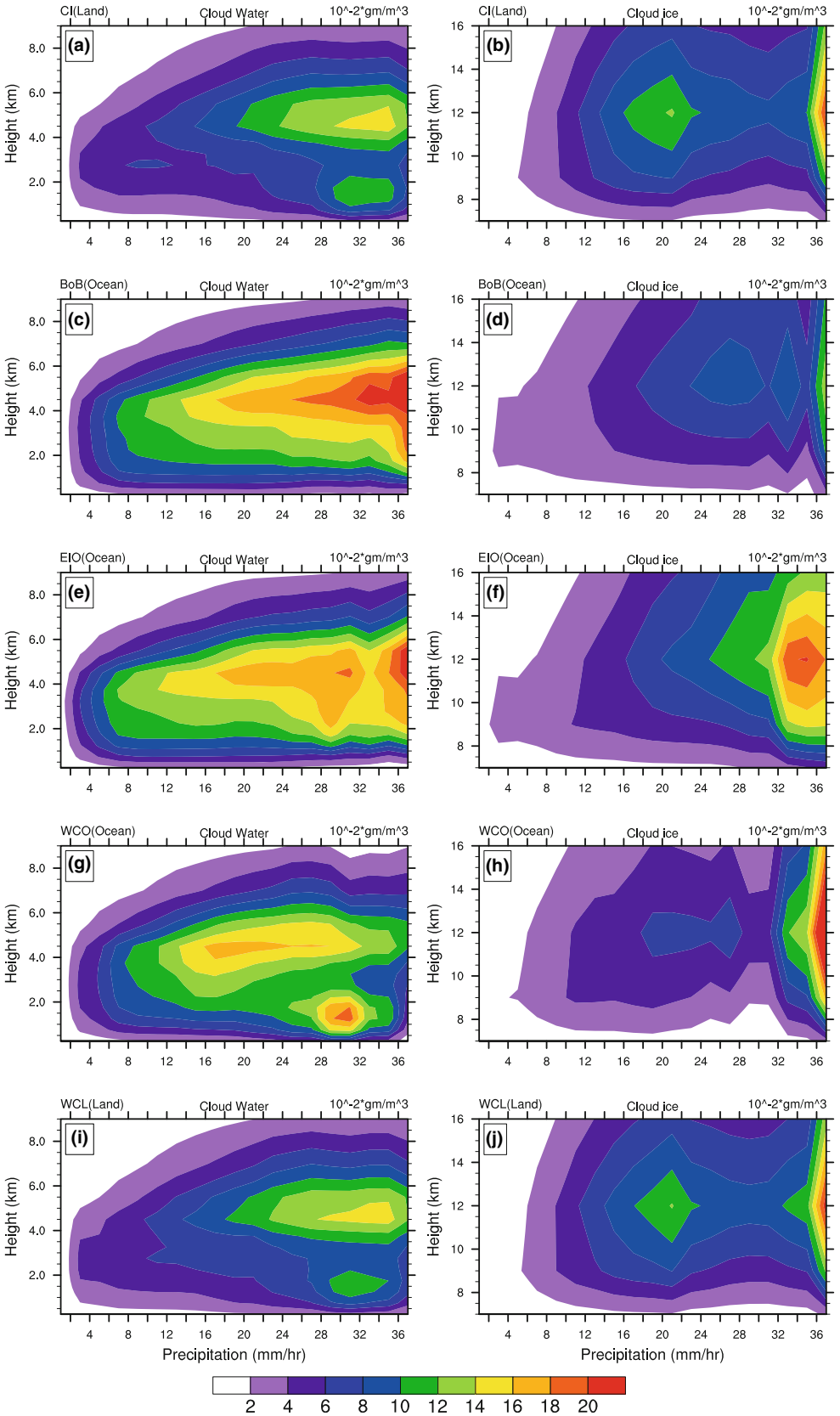

Fig. 3 Vertical mean distribution of observed (TRMM 2A12; JJAS 2004–2010) CLW (*left column*) and CLI (*right column*), as a function of precipitation, over **a**, **b** CI; **c**, **d** BoB; **e**, **f** EIO; **g**, **h** WCO; and **i**, **j** WCL. The precipitation values have been grouped into 2 mm/h bins

the vertical) at 1.5 and 5 km. The presence of two maxima could perhaps be better understood by the fact that the probability of occurrence of multilayer clouds over the Indian region is ≈50 % (e.g., Luo et al. 2009).

Figure 3c, e and g show the CLW distributions for oceanic regions. We find that the orographically influenced region (WCO; Fig. 3g) behaves differently from open ocean (EIO; Fig. 3e) and trapped ocean (BoB; Fig. 3c). Specifically, the lower rainfall ranges (<25 mm/h) have more CLW than higher rainfall ranges in WCO (Fig. 3g) as compared to EIO and BoB where the behaviour is the opposite. CLI, on the other hand, is higher over EIO (Fig. 3f) compared to BoB (Fig. 3d) and WCO (Fig. 3h) for precipitation intensities greater than 20mm/hr. In general, it appears that CLI profiles show a maximum in the vertical distribution for higher values of rainfall. On the one hand, the higher intensities of rainfall are likely to be due to deep convection, often associated with tall clouds with anvil, leading thus to high values of CLI; this suggests that the high amount of CLI might be realistic (and not just a by-product of biases in TRMM 2A12). On the other hand, since the number of samples is very small at intensities higher than 30 mm/h, the uncertainty in CLI at high rainrates is also likely to be very high.

In summary, it appears that land regions (orographically influenced or not) show very similar CLW and CLI structure; however, over oceans, the behaviour is a bit more complex. While the trapped (BoB) and open (EIO) ocean region CLW and CLI distributions appear to be similar to each other, the orographically influenced ocean region (WCO) has CLW and CLI profiles between those of land and ocean.

3.2 Seasonal differences

Having seen geographical differences in terms of separation of CLW and CLI profiles over land and ocean regions, we turn our attention to temporal differences. Specifically, we attempt to document any differences in the structure of CLW during the monsoon season as well as between monsoon and premonsoon periods.

Our analysis here focuses exclusively on central India, as it is a region directly affected by monsoon intraseasonal oscillations. Figure 4 shows the vertical profile of climatological (2004–2010) mean cloud liquid water during premonsoon (May) and monsoon (JJAS) periods. While Fig. 4a is the mean estimated from all grids (i.e., with and without surface precipitation), Fig. 4b shows vertical structure of CLW only for those grids with measurable rainfall. It is quite clear that when all grids/days are considered, the mean CLW, as expected, is higher for the monsoon season compared to the premonsoon season. However, the opposite is true if only rainy grids/days are considered, namely, that the surface rainfall in the premonsoon season (May) originates from clouds with higher value of CLW as compared to monsoon season (JJAS).

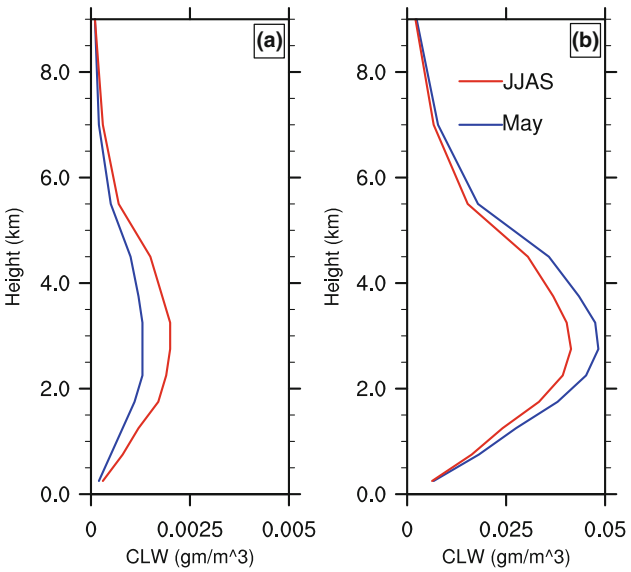

Fig. 4 Vertical profiles of climatological (2004–2010) mean cloud liquid water (gm/m^3) for May (*blue*), JJAS (*red*) over central India for **a** for all grids/days, **b** for only those grids/days with measurable rain

Figure 5a shows the difference in vertical profiles of CLW at different (non-zero) precipitation intensities between May and JJAS over central India. The hatched region on this figure indicates differences which are statistically significant at 5 % level. It is evident from this figure that while the differences in CLW between the premonsoon and monsoon season are significant at lower rainfall intensities, at higher intensities (≈above 20 mm/hr), the differences are statistically not significant. Figure 5b shows the differences in vertical profiles of CLW during June (early monsoon) and August (late/peak monsoon). Note that in both these figures the significant differences are only for rainfall intensity less than 20 mm/hr. In addition, the CLW during May (June) is higher than during JJAS (August). Therefore, Fig. 5, taken as a whole, suggests that the CLW during periods of low precipitation (May or June) is higher than that during periods of high precipitation (JJAS or August). This appears to be contradictory to what was seen earlier in Fig. 2c which pointed to a monotonically increasing relation between CLW and precipitation. However, our contention is that the higher CLW during the premonsoon or early monsoon could potentially be associated with the high aerosol concentration typically observed during May over central India compared to the monsoon season (e.g., see Fig. 1b or 3 in Gautam et al. 2009). This could also explain why the difference between May and JJAS CLW is higher in magnitude than the difference between June and August CLW.

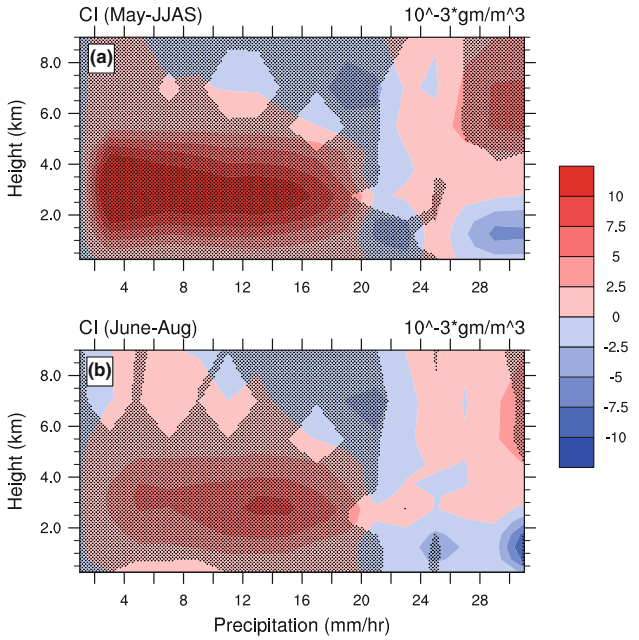

Fig. 5 Vertical mean distribution of the difference between observed (TRMM 2A12; 2004-2010) CLW during **a** May and JJAS; **b** June and August, as a function of precipitation, over central India. The hatched region corresponds to differences significant at 5 % significance level

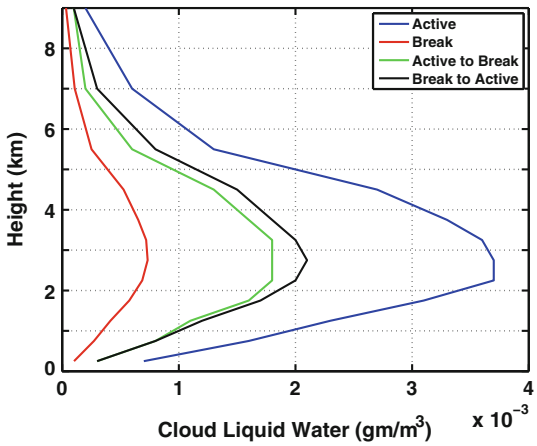

Fig. 6 Vertical profiles of climatological (2004–2010) mean cloud liquid water (gm/m^3) for active (*blue*), break (*red*), active-to-break (*green*) and break-to-active (*black*) phases during JJAS over central India

The indirect effect of aerosol (acting as cloud condensation nuclei) is an issue we will explore later in this section.

Noting that, during the monsoon season, the most prominent signatures are the active and break phases, generally associated with the northward movement of the intertropical convergence zone, we focus on the vertical structure of CLW during these phases. In this study, the active and break phases of the monsoon are defined as follows: When the daily rainfall during a monsoon season is more (less) than $\mu + 0.5\,\sigma$ ($\mu - 0.5\,\sigma$) for a period of at least three consecutive days, then that period is called active (break) phase. Here, μ and σ refer to the seasonal mean and standard deviation of rainfall. In addition to the active and break phases, two new phases are also identified, namely, active-to-break and break-to-active phases. These are transition phases just prior to the beginning of a break or an active phase.

Figure 6 shows the vertical profiles of the CLW for these four different phases of monsoon (active, break, break-to-active, and active-to-break phases) over CI. The mean CLW is maximum in the active phase and minimum in the break phase; these features match with the results reported by Rajeevan et al. (2012) using Cloudsat data. We also find that the break-to-active transition phase has greater mean CLW than that of the active-to-break transition phase.

The vertical distribution of the climatological difference between the CLW during active-to-break and break-to-active transition phases and between active and break phases over central India, as a function of precipitation, is shown in Fig. 7a, b. Figures 7c, d show the precipitation frequency histograms during each of the phases, which provides an estimate of the number of samples used in assessing significant differences (hatched regions). This distribution clearly indicates that the break-to-active transition phase has significantly higher CLW than during the active-to-break phase (hatched region in Fig. 7a). Interestingly, even though the break phase has lower amount of mean CLW (Fig. 6), it has higher amount of CLW for lower precipitation intensities (<20 mm/hr) than in the active phase (Fig. 7b).

In order to understand further the differences in CLW profiles during active and break phases, over central India, we compare the temporal variation of rainfall and mean optical depth, an indicator of aerosol concentration. Figure 8a shows the 5-days running mean rainfall (TRMM 3B42) and the mean aerosol optical depth (Moderate Resolution Imaging Spectroradiometer: MODIS/Terra) for JJAS of 2009 over central India. This particular year is chosen to exaggerate the out of phase behaviour between AOD and rain over central India. It is evident from the figure that during the break phase, the value of mean optical depth increases (e.g., end of July, early August). We argue here that this increase in aerosol concentration during no-rain conditions results in greater CLW in the atmosphere due to the aerosol indirect effect (Panicker et al. 2010). At a more quantitative level, we consider all the active-to-break and break-to-active phases for the seven consecutive monsoons (2004–2010). Figure 8b shows the frequency distributions of AOD (only for days when rain exceeds 1 mm/day) for the two phases. While the modes of the AOD distributions for both phases are nearly the same, the active-to-break transition has significantly higher

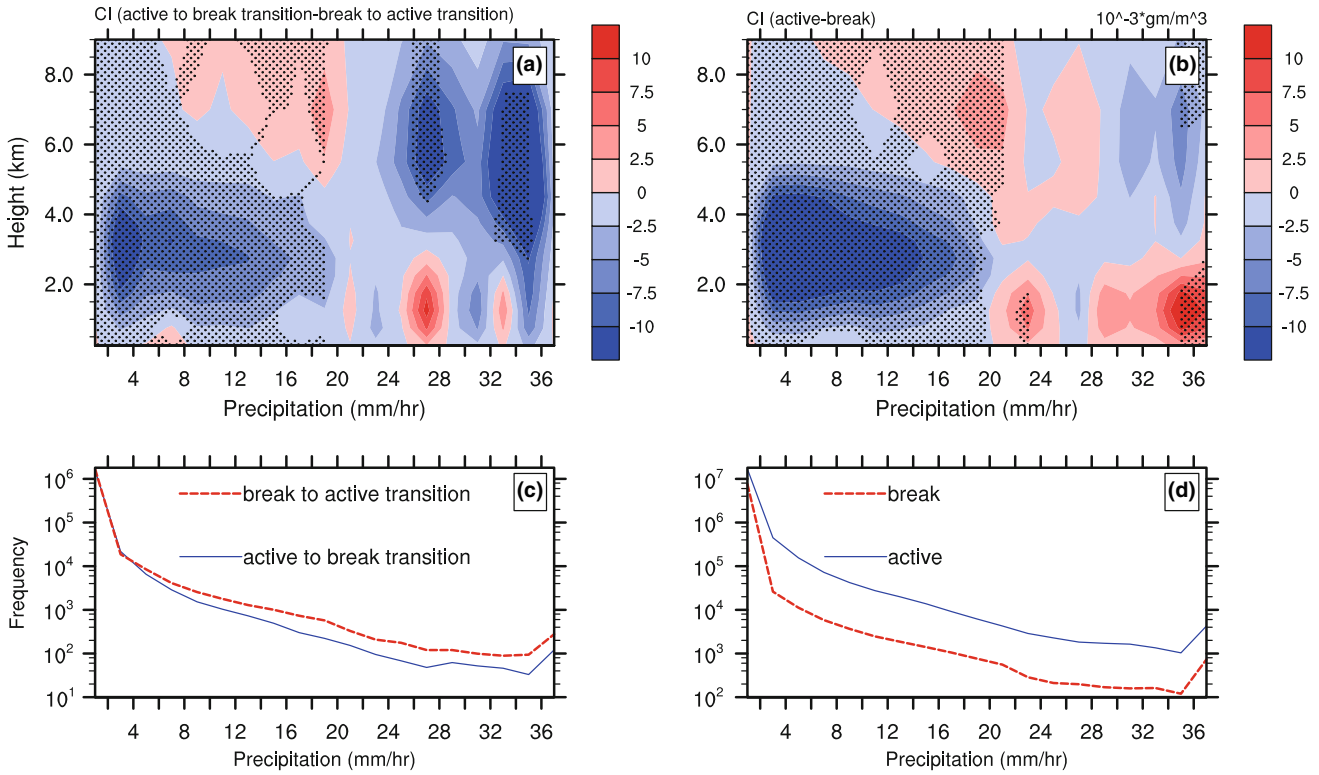

Fig. 7 (*Top row*) Vertical mean distribution of difference between observed (TRMM 2A12; JJAS; 2004–2010) CLW in **a** active-to-break and break-to-active transition; **b** active and break phases of the monsoon, as a function of precipitation, over central India. The hatched region corresponds to differences significant at 5 % significance level. (*Bottom row*) **c**, **d** Frequency distribution of precipitation during the four phases, indicating the number of samples that have been used in assessing the significant differences

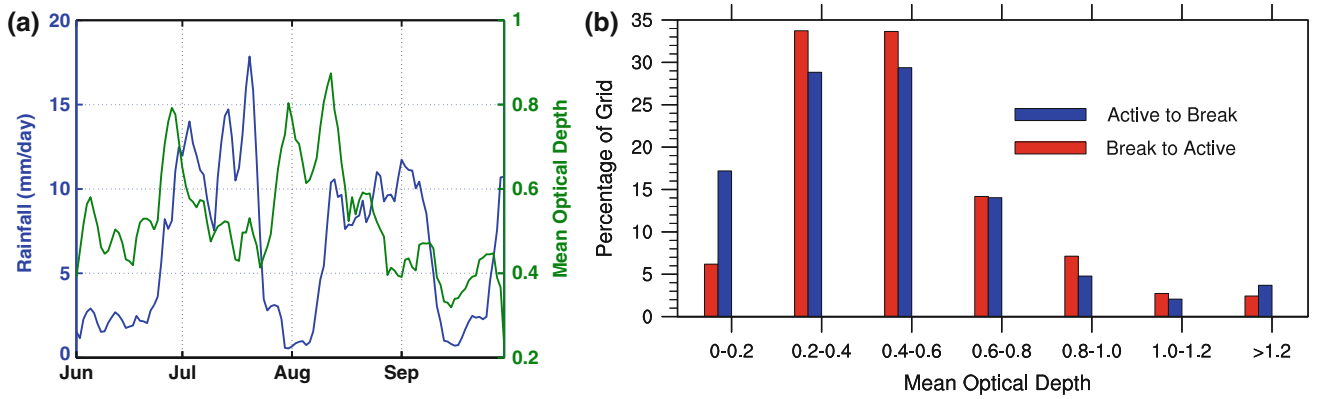

Fig. 8 **a** Five days (running) mean rainfall (TRMM 3B42) and mean aerosol optical depth (MODIS terra data) during JJAS of 2009 over central India; and **b** Normalised frequency distribution of mean optical depth over the same region during break to active (*red*) and active to break (*blue*) phases of monsoon

occurrence of low mean optical depth, coupled with more instances of higher optical depth during the break-to-active phase. This demonstrates that the mean AOD value, an indicator of aerosol concentration, is higher during the break to active transition phase compared to the active to break phase. Preliminary analysis suggests that there is a significant negative correlation (~ -0.6) between the intraseasonal timescales (30–60 days filtered anomalies) of AOD and rain.

The assertion above is further verified when a similar analysis is done for a nearby region, with a different amount of atmospheric aerosol loading. Figure 9 shows total column aerosol optical depth from MODIS during JJAS of 2004–2010 over Central India (the region under

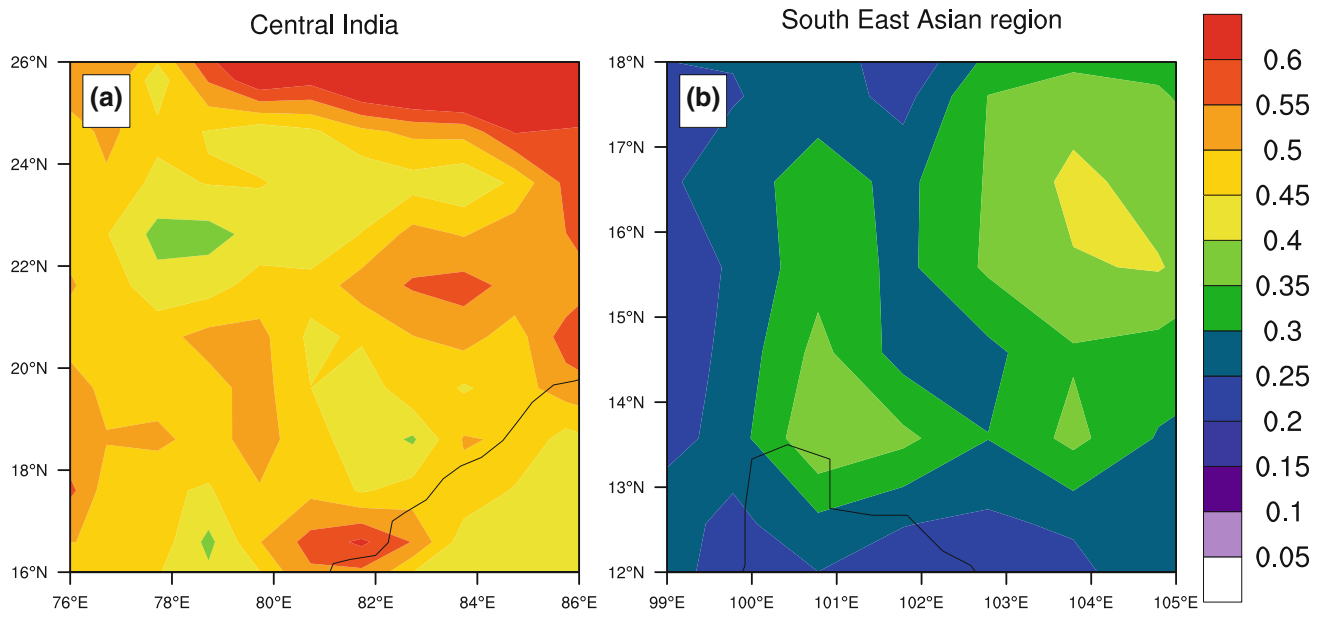

Fig. 9 Spatial distribution of the climatological (2004–2010) mean aerosol optical depth during the monsoon season (JJAS) over **a** central India; and **b** a region over southeast Asia

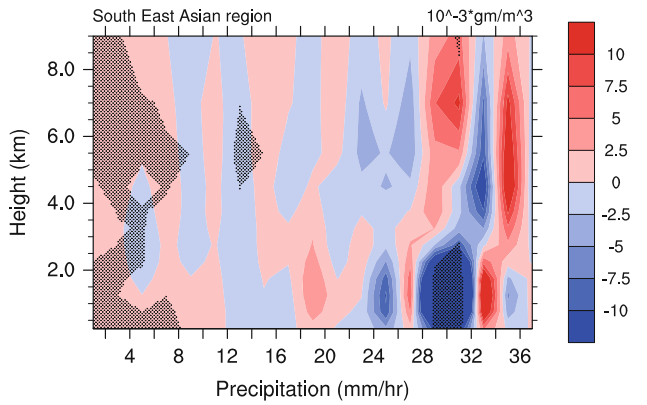

Fig. 10 Vertical mean distribution of difference in observed (TRMM 2A12; JJAS 2004–2010) CLW between the active-to-break and break-to-active transition phases of monsoon, as a function of precipitation, over southeast Asia (99–105E, 12–18N). The differences significant at 5 % significance level are hatched

consideration in Figs. 7, 8) and southeast Asia (land part of 99–105E, 12–18N). Note that, aerosol optical depth over southeast Asia, on an average, is almost half to that over central India during this season. Figure 10 shows the vertical mean distribution of the difference in the observed CLW between the active-break transition phases over southeast Asia. Unlike over central India (Fig. 7a), southeast Asia did not show any significant difference in CLW during break-to-active transition phase as compared to active-to-break transition phase. This might be due to the fact that this region has much less aerosol as compared to central India. More aerosols in the atmosphere are likely to act as cloud condensation nuclei and give rise to more number of smaller droplets. Smaller droplets are less likely to grow to the size of a rain-drop through collision-coalescence procedure and increase CLW of the atmosphere. The evidence presented above relating AOD and CLW or rain is only an attribution, and a more thorough investigation with the help of numerical models is needed to corroborate this hypothesis.

4 Conclusions

The vertical structure of hydrometeors over the Indian region and the surrounding oceans is not well documented due to limited observations. Using TRMM 2A12 microwave estimates of cloud liquid water and cloud ice for 7 years (2004–2010), we systematically document the vertical distribution of cloud liquid water and cloud ice over the Indian land and surrounding ocean regions, and attempt to understand some of the observed geographical and seasonal differences. In general, we find that the mean cloud liquid water and cloud ice content of land and oceanic regions are different, with the ocean regions showing higher amount of CLW. This difference could partly be attributed to known biases (especially over oceans) in 2A12 Version-6 data set. A recent version of 2A12 (Version-7) uses total column water vapor as an additional parameter to retrieve CLW and CLI, and purportedly reduces the biases (at least of surface precipitation over oceans; see Kummerow et al. 2011). The role of biases aside, the higher value of CLW over the Bay of Bengal in comparison to central Indian region seems to be consistent with the characteristics of

outgoing longwave radiation (e.g., more instances of deep convection over BOB than over central India). This suggests that the relative contribution of the known biases in TRMM 2A12 and regional behavior in determining the observed ocean-land contrast is an issue that needs further investigation. We also find that the western parts of the Indian region show a striking land-sea contrast. While the CLW and CLI over the land part of the Arabian Sea coast (WCL) have similar distribution as those of central India, the CLW and CLI profiles over the oceanic part (WCO) are higher than the profiles for the land regions and lower than profiles for the Bay of Bengal (trapped ocean) and the equatorial Indian Ocean (open ocean) regions. Specifically, at relatively low rainfall intensities, we find higher amount of CLW over the Arabian Sea than over the Bay of Bengal and the equatorial Indian Ocean. The converse is true for high rainfall regimes. In addition, we find for both land and ocean, CLW and CLI have a monotonically increasing relation with precipitation intensity, albeit with high uncertainty at high rainrates.

When interseasonal (monsoon vs. premonsoon) or intraseasonal (June vs. August) CLW profiles are compared, the lower rainfall periods (May and June) appear to show higher CLW than the higher rainfall periods (JJAS or August). We speculate that the higher CLW during the lean rainfall periods could potentially be attributed to the indirect aerosol effect, considering the fact that May and June mean aerosol optical depths are significantly higher (suggesting higher aerosol concentration) than during the monsoon season. Specifically, during the break phase, due to increased heating, aerosols (e.g., black carbon) are generated in the region. As a consequence, the indirect effect of aerosols is to provide favourable conditions (i.e., acting as cloud condensation nuclei) for larger accumulation of cloud liquid water. We tested this speculation by comparing CLW over central India with a region close to the Indian subcontinent, namely, southeast Asia, which does not have significant aerosol loading. Preliminary analysis suggests that our speculation has value. In particular, unlike the central Indian region, where the CLW in the break-to-active transition phase is significantly higher than in the active-to-break transition phase, the southeast Asian region shows no significant difference in the CLW profiles across different phases of the monsoon. Clearly, a more thorough investigation is needed with the aid of numerical models to corroborate the hypothesis.

Acknowledgments The data used in this study were acquired as part of the NASA's Earth-Sun System Division and archived and distributed by the Goddard Earth Sciences (GES) Data and Information Services center (DISC). Discussions with Robert Houze Jr. and Guosheng Liu are gratefully acknowledged. AC and VV acknowledge funding from the Continental Tropical Convergence Zone (CTCZ) programme under the Ministry of Earth Sciences, Govt. of India. We thank two anonymous reviewers for their insightful comments, which helped improve the manuscript.

References

Berg W, L'Ecuyer T, Kummerow C (2006) Rainfall climate regimes: the relationship of regional TRMM rainfall biases to the environment. J Appl Meteor Climatol 45:434–454. doi:10.1175/JAM2331.1

Dinku T, Anagnostou EN (2005) Regional differences in over land rainfall from PR-calibrated TMI algorithm. J Appl Meteor 44:189–205. doi:10.1175/JAM2186.1

Gautam R, Hsu NC, Lau KM, T MK (2009) Aerosol and rainfall variability over the Indian monsoon region: distributions, trends and coupling. Ann Geophys 27:3691–3703

Gopalan K, Wang NY, Ferraro R, Liu C (2010) Status of the TRMM 2A12 land precipitation algorithm. J Atmos Ocean Technol 27:1343–1354. doi:10.1175/2010JTECHA1454.1

Halder M, Mukhopadhyay P, Halder S (2012) Study of the microphysical properties associated with the Monsoon Intraseasonal Oscillation as seen from the TRMM observations. Ann Geophys 30:897–910. doi:10.5194/angeo-30-897-2012

Houze RA (1982) Cloud clusters and large-scale vertical motions in the tropics. J Meteor Soc Jpn 60:396–410

Kummerow C, Hong Y, Olson W, Yang S, Adler R, McCollum J, Ferraro R, Petty G, Shin DB, Wilheit T (2001) The evolution of the Goddard Profiling Algorithm (GPROF) for rainfall estimation from passive microwave sensors. J Appl Meteorol 40(11):1801–1820

Kummerow CD, Ringerud S, Crook J, Randel D, Berg W (2011) An observationally generated a priori database for microwave rainfall retrievals. J Atmos Ocean Technol 28(2):113–130

Luo Y, Zhang R, Wang H (2009) Comparing occurrences and vertical structures of hydrometeors between eastern China and the Indian monsoon region using CloudSat/CALIPSO data. J Clim 22(4):1052–1064

Marchand R, Mace GG, Ackerman T, Stephens G (2008) Hydrometeor detection using CloudsatAn earth-orbiting 94-GHz cloud radar. J Atmos Ocean Technol 25:519–533. doi:10.1175/2007JTECHA1006.1

Masunaga H, Iguchi T, Oki R, Kachi M (2002) Comparison of rainfall products derived from TRMM Microwave Imager and Precipitation Radar. J Appl Meteor 41:849–862

Matsuno T (1966) Quasi-geostrophic motions in the equatorial area. J Meteor Soc Jpn 44:25–43

Noh YJ, Haar HV (2009) Comparison and validation of WRF-ARW cloud microphysics schemes during C3VP/CLEX-10 field experiment. In: 10th WRF Users' Workshop in Boulder Colorado, 23–26 June 2009

Olson WS, Kummerow CD, Yang S, Petty GW, Tao WK, Bell TL, Braun SA, Wang Y, Lang SE, Johnson DE, Chiu C (2006) Precipitation and latent heating distributions from satellite passive microwave radiometry. Part I: improved method and uncertainties. J Appl Meteor Climatol 45:702–720. doi:10.1175/JAM2369.1

Panicker AS, Pandithurai G, Dipu S (2010) Aerosol indirect effect during successive contrasting monsoon seasons over Indian subcontinent using MODIS data. Atmos Environ 44:1937–1943. doi:10.1016/j.atmosenv.2010.02.015

Rajeevan M, Rohini P, Niranjan Kumar K, Srinivasan J, Unnikrishnan CK (2012) A study of vertical cloud structure of the Indian summer monsoon using CloudSat data. Clim Dyn 1–14. doi:10.1007/s00382-012-1374-4

Tao WK, Lang S, Olson WS, Meneghini R, Yang S, Simpson J, Kummerow C, Smith E, Halverson J (2001) Retrieved vertical

profiles of latent heat release using TRMM rainfall products for February 1988. J Appl Meteor 40:957–982
Wang NY, Liu C, Ferraro R, Wolff D, Zipser E, Kummerow C (2009) TRMM 2A12 land precipitation productstatus and future plans. J Meteor Soc Jpn 87A:237–253
Webster PJ (1972) Response of tropical atmosphere to local, steady forcing. Mon Weather Rev 100:518–541
Zuluaga MD, Hoyos CD, Webster PJ (2010) Spatial and temporal distribution of latent heating in the South Asian monsoon region. J Clim 23:2010–2029. doi:10.1175/2009JCLI3026.1